ChemComm

Accepted Manuscript

ROYAL SOCIETY OF CHEMISTRY

rsc.li/chemcomm

View Article Online
DOI: 10.1039/C9CC04300D

COMMUNICATION

Construction of fluorescent probe for selectively detecting singlet oxygen with high sensitivity and large concentration range based on two-step cascade sensing reaction

Received 00th January 20xx,
Accepted 00th January 20xx

DOI: 10.1039/x0xx00000x

Lingliang Long,*[a] Xiangqi Yuan,[a] Siyu Cao,[a] Yuanyuan Han,[a] Weiguo Liu,[a] Qian Chen,[a] Aihua Gong,*[b] and Kun Wang*[a,c]

A novel fluorescent probe XQ-1 for selectively detecting $^1O_2$ on the basis of two-step cascade reaction has been rationally constructed. The probe responded to $^1O_2$ not only showing high sensitivity, but also displaying large concentration range, which renders the probe can be used as a powerful tool to monitor the efficacy of PDT to cancer and concurrently track the adverse effect to healthy cells.

Singlet oxygen ($^1O_2$) is a selectively reactive oxygen species (ROS) and plays significant roles in a variety of physical, chemical, biological, and medical events.[1] Particularly, the $^1O_2$ is appealing in recent medical studies due to it exerts main effect on photodynamic therapy (PDT), a minimally invasive methodology for anticancer treatment.[2] In the process of PDT treatment, upon selective photoirradiation of the cancer region, the non-toxic photosensitizers (PS) and oxygen cause the production of $^1O_2$ that can give a cytotoxic activity toward cancer cells.[3] Nevertheless, the PDT is essentially an intricate process. The $^1O_2$ concentration is drastically varied during the PDT treatment, due to the PS distribution, photoirradiation fluence rate, and oxygen concentration change dynamically and interdependently in different individuals.[4] Over the past few years, understanding the biology of PDT has expanded, however, it remains challenging to detect $^1O_2$ concentration and track the related dynamics, which is extremely crucial for achieving optimal efficacy and safety of PDT treatment in clinic, especially when there is curative intent. Consequently, construction of an efficient method for detecting the $^1O_2$ concentration during the PDT treatment is of great significance.

Among a variety of strategies for detection of $^1O_2$, fluorescent probe seems to be a superb tool for monitoring $^1O_2$ in biological system owing to their features of high sensitivity, simplicity, non-invasiveness and potential for in vivo imaging.[5] Currently, several fluorescent probes with fluorescein, rhodamine and europium complex as fluorophore and 9,10-disubstituted anthracene as $^1O_2$ trap have been developed.[6] Very few fluorescent probes using furan[7] and histidine[8] as $^1O_2$ trap were also constructed. Zhang et al designed mitochondria targeted probe for detecting $^1O_2$ during the PDT process.[9] Moreover, chemiluminescence probes with enol-ether or anthracene as $^1O_2$ trap were judiciously developed.[10] Nonetheless, these reported probes for detection of $^1O_2$ during the PDT process were still retarded by their properties of either small concentration range or low sensitivity. Previous studies presented that the threshold dose of $^1O_2$ in PDT process was varied over a large range from 0.1 mM to 12.1 mM.[11] Thus, a fluorescent probe responding to $^1O_2$ with a large concentration range is beneficial to monitor the efficacy of PDT treatment. On the other hand, during the process of PDT treatment, the scattered light may lead to producing small dosage of $^1O_2$ in the healthy cells adjacent to the cancer cells. The elevated levels of $^1O_2$ will induce severe damage to the healthy cells, since the $^1O_2$ can irreversibly oxidize various kinds of biological molecules such as DNA, proteins, and lipids.[12] Therefore, to prevent the adverse effect of PDT treatment to healthy cells, fluorescent probe should also display sufficient sensitivity to monitor small dosage of $^1O_2$ in the surrounding healthy cells. However, in general, a fluorescent probe in response to analyte with large concentration range is hard to respond to the analyte with high sensitivity, or vice versa. Therefore, development of a fluorescent probe for $^1O_2$ not only displaying large concentration range, but also showing high sensitivity is a great challenge, but in urgent demand.

Herein, we rationally developed an anthracene fluorophore conjugated quinolinium, **XQ-1**, as a novel fluorescent probe for $^1O_2$ (Scheme 1). Remarkably, probe **XQ-1** was able to detect the $^1O_2$ on the basis of two-step cascade sensing reaction. The first step sensing

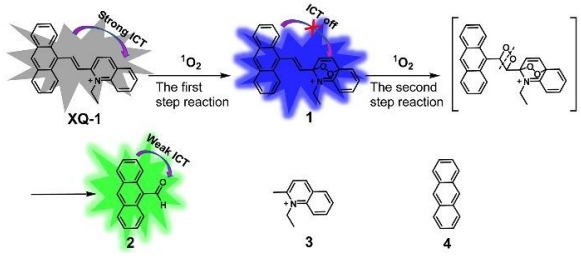

Scheme 1 The sensing reaction of probe **XQ-1** to $^1O_2$ based on two-step cascade sensing reaction, and the chemical structure of compound **3** and **4**.

[a] School of Chemistry and Chemical Engineering, Jiangsu University, Zhenjiang, Jiangsu 212013 (P. R. China). E-mail: longlingliang@163.com, wangkun@ujs.edu.cn
[b] School of Medicine, Jiangsu University, Zhenjiang, Jiangsu 212013, (P. R. China). E-mail: ahg5@ujs.edu.cn
[c] Key Laboratory of Optic-electric Sensing and Analytical Chemistry for Life Science, Ministry of Education, College of Chemistry and Molecular Engineering, Qingdao University of Science and Technology, Qingdao, Shandong 266042 (P. R. China).
† Footnotes relating to the title and/or authors should appear here.
Electronic Supplementary Information (ESI) available: [details of any supplementary information available should be included here]. See DOI: 10.1039/x0xx00000x

DOI: 10.1039/C9CC04300D

reaction makes the probe detect $^1O_2$ with high sensitivity, and the second step sensing reaction renders the probe detect $^1O_2$ with large concentration range.

The synthesis and characterization of the probe **XQ-1** were displayed in supporting information (Scheme S1). The fluorescence responses of probe **XQ-1** to $^1O_2$ were observed in blue fluorescence channel and green fluorescence channel. In the absence of $^1O_2$, probe **XQ-1** displayed almost no fluorescence (Φ_F = 0.004) in both blue channel (Fig. 1a) and green channel (Fig. 1b). The quenched fluorescence was probably attributed to the strong intramolecular charge transfer (ICT) process from anthracene fluorophore to quinolinium moiety.[13] To illustrate these phenomena, time-dependent density functional theory (TD-DFT) calculations were carried out. The HOMO→LUMO transition ($S_0 \rightarrow S_1$) in probe **XQ-1** was allowable (*f*=0.4866), which showed that the electron on the anthracene fluorophore was almost completely transferred to the quinolinium moiety (Fig S1), implying the strong ICT. In addition, the $S_1 \rightarrow S_0$ transition is forbidden (*f*=0.0000), which means that probe **XQ-1** is essentially nonfluorescent.

The responses of probe **XQ-1** to $^1O_2$ were investigated using MoO_4^{2-}/H_2O_2 system as the $^1O_2$ source, as one $^1O_2$ molecule can be quantitatively generated by reaction of two H_2O_2 under the catalysis of MoO_4^{2-}.[14] When a small dosage of $^1O_2$ (0-0.6 mM) was introduced, the fluorescence of probe **XQ-1** (20 μM) displayed dramatic enhancement in the blue channel (Φ_F = 0.184) (Fig. 1a, 1e), and almost no fluorescence variations were noted in the green channel (Fig. 1b). Thus, the sensing reaction was occurred after the probe treated with a small dosage of $^1O_2$. Moreover, the profiles of fluorescence emission spectra and excitation spectra in the blue channel were resembled to that of anthracene **4** (Fig. S2, S3). These results suggested that the anthracene fluorophore in the sensing reaction product was intact. Furthermore, the results also inferred that the strong ICT process from anthracene to quinolinium moiety in the sensing reaction product was interrupted, which leads to the recovery of anthracene fluorescence. The tremendous fluorescence enhancement in blue channel upon treatment with a small dosage of $^1O_2$ made probe **XQ-1** sense $^1O_2$ with high sensitivity. As shown in Fig. S4, the fluorescence intensity in the blue channel (I_{412}) showed linear relationship with the dosage of $^1O_2$ in the range from 0 mM to 0.45 mM. And the detection limit was calculated to be 0.138 μM (S/N = 3).

Interestingly, when more dosages of $^1O_2$ were added (0.6 mM-50 mM), the enhanced fluorescence in the blue channel set out to attenuate (Fig. 1c). Meanwhile, an intense fluorescence in the green channel centered at 506 nm was emerged and progressively increased (Φ_F = 0.138) (Fig. 1d, 1f). These deduced that the first sensing reaction product further reacted with $^1O_2$ to produce another fluorescent product. The fluorescence intensity at 506 nm showed good linear relationship with the logarithm of various dosage of $^1O_2$ in the range of 0.6 mM to 50 mM (Fig. S5). Thus, probe **XQ-1** also exhibited fluorescence response to $^1O_2$ with very large concentration range, which is beneficial to monitor the efficacy during the PDT treatment. In addition, probe **XQ-1** displayed similar fluorescence response when the $^1O_2$ was generated from photoirradiation of PS **TMPyP4** (5 μM) (Fig. S6-S7).

In view of the fluorescence response of probe **XQ-1** to $^1O_2$, we can conclude that two-step cascade sensing reaction would be involved in probe **XQ-1** detecting $^1O_2$. To further explore the sensing mechanism, we tried to isolate and characterize the two sensing reaction products. However, the first step sensing reaction product was unstable in the process of isolation, which is frequently found in $^1O_2$ related reaction products.[10a, 15] Fortunately, an ESI-Ms spectra

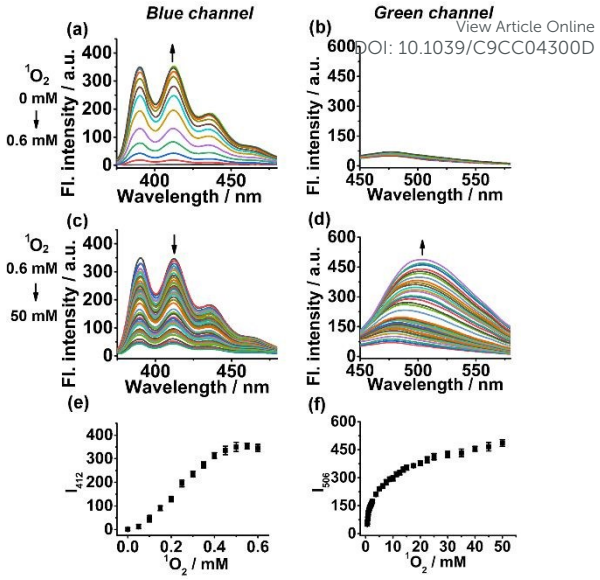

Fig. 1 Changes in fluorescence spectra of probe **XQ-1** (20 μM) with 0-0.6 mM $^1O_2$ in blue channel (λ_{ex} = 368 nm) (a) and green channel (λ_{ex} = 420 nm) (b); Changes in fluorescence spectra of probe **XQ-1** with 0.6-50 mM $^1O_2$ in blue channel (λ_{ex} = 368 nm) (c) and green channel (λ_{ex} = 420 nm) (d); Changes in fluorescence intensity at 412 nm of probe **XQ-1** with 0-0.6 mM $^1O_2$ (e); Changes in fluorescence intensity at 506nm of probe **XQ-1** with 0.6-50 mM $^1O_2$ (f). The error bars represent the standard deviation (n = 3).

was acquired when the probe was directly reacted with $^1O_2$ in the period of first step reaction (Fig. S8). According to the ESI-Ms spectra, together with the aforementioned fluorescence spectra and the chemical reaction of $^1O_2$,[16] we tentatively proposed compound **1** as the possible first step sensing reaction product (Scheme 1). In this product, quinolinium moiety was broken by an 1,4-cycloaddition reaction with $^1O_2$, and thus the strong ICT process between anthracene moiety and quinolinium moiety was blocked, which induced the fluorescence recovery of anthracene fluorophore. The second step sensing reaction product was successfully isolated, and the structure was identified to be compound **2** according to the ^1H NMR spectroscopy (Fig. S9), ESI-Ms spectra (Fig. S10), fluorescence emission spectra (Fig. S11), and fluorescence excitation spectra (Fig. S12). Based on the molecular structure of compound **2**, a 1,2-cycloaddition reaction would be associated with the second step sensing reaction (Scheme 1). In addition, compared with the fluorescence of compound **1** in the blue channel, the fluorescence of compound **2** was red-shifted to the green channel. The red-shifted fluorescence was attributed to weak ICT transition from anthracene moiety to the aldehyde moiety, which was illustrated by TD-DFT calculation (Fig. S13). Therefore, the novel fluorescent probe could detect $^1O_2$ in two distinct fluorescence channels on the basis of the two-step cascade reaction. This makes the probe detect $^1O_2$ with both high sensitivity and large concentration range.

The UV-Vis absorption spectra responses of probe **XQ-1** to $^1O_2$ were inspected. Probe **XQ-1** itself exhibited two main absorption peaks at 478 nm and 331 nm, respectively (Fig. S14). The broad absorption peak at 478 nm is apparently ascribed to the transition of ICT process from anthracene fluorophore to quinolinium moiety. The absorption peak at 331 nm was due to the π-π* transition in the quinolinium moiety. This can be illustrated by the TD-DFT calculation. As shown in Fig S1, the HOMO-4→LUMO transition (*f* = 0.2266) is the π-π* transition in the quinolinium moiety, which is responsible for the absorption peak at 331 nm. Moreover, by comparing the UV-Vis absorption spectra of probe **XQ-1** with that of *N*-ethyl-2-

methylquinolinium iodide **3** (Fig. S15), the absorption at 331 nm was confirmed to be originated from the π-π* transition in the quinolinium moiety. After treatment with small dosage of $^1O_2$ (0-0.6 mM), the absorption peak at 478 nm decreased, denoting that the strong ICT process from anthracene fluorophore to quinolinium moiety was inhibited. Concomitantly, the absorption peak at 331 nm was also decreased, inferring that the quinolinium structure was broken, consistent with the structure of the proposed compound **1**. After reaction with 0.6 mM $^1O_2$, several weak absorption peaks were observed at 388 nm, 369 nm, 345 nm, and 326 nm, respectively. These peaks are attributed to the π-π* transition of anthracene (Fig. S16). When more dosage of $^1O_2$ (0.6 mM-50 mM) was introduced, a broad absorption peak at 409 nm was increased (Fig. S17), which was ascribed to the transition of weak ICT process from the anthracene to aldehyde in compound **2** (Fig. S13). Therefore, the variation of the absorption spectra of probe **XQ-1** to $^1O_2$ further demonstrated the two-step cascade sensing reaction.

To examine the detection specificity of probe **XQ-1** to $^1O_2$, **XQ-1** was treated with 0.6 mM various relevant species including reactive oxygen species and metal ions. As displayed in Fig. S18, only $^1O_2$ could trigger obvious fluorescence enhancement at 412 nm, while other species did not induce any spectral changes. Furthermore, the fluorescence color changes of **XQ-1** to various species indicated that **XQ-1** was able to detect $^1O_2$ by naked eyes. These results revealed that the probe showed a highly selective response to $^1O_2$. The influence of pH value on the fluorescence response of **XQ-1** to $^1O_2$ was explored (Fig. S19). **XQ-1** was capable of detecting $^1O_2$ within the pH range of 7-12, denoting that **XQ-1** worked well at physiological and alkaline pH condition. The effect of water volume fraction on **XQ-1** sensing $^1O_2$ was also studied (Fig. S20). **XQ-1** can be used for detecting $^1O_2$ even in the solution with 70% water. The photostability of **XQ-1** to $^1O_2$ was further inspected. The results denoted that the enhanced fluorescence in the blue channel and green channel was stable under photoirradiation (Fig. S21-S22). In addition, the *pseudo*-first-order rate constant (k') was determined to be 0.04457 min^{-1} and 0.10379 min^{-1} for the probe reacted with 0.6 mM $^1O_2$ and 50 mM $^1O_2$, respectively (Fig. S23-S24).

To examine whether the probe is sufficiently sensitive to detect small dosage of $^1O_2$ in living system, probe **XQ-1** was employed for fluorescence imaging of endogenous $^1O_2$ in RAW 264.7 macrophage cells. After stained with 2 μM **XQ-1** at 37°C for 30 min, the cells exhibited negligible background fluorescence in blue channel (Fig. 2a) and green channel (Fig. 2e). When **XQ-1** stained cells were further incubated with increasing dosage of phorbol myristate acetate (PMA, an activator for endogenous $^1O_2$ production),[17] the fluorescence in blue channel enhanced correspondingly (Fig. 2b-2c, 2m). Moreover, in a control experiment, **XQ-1** stained cells were pre-treated with histidine (His, a $^1O_2$ scavenger),[18] and then incubated with PMA. No visible fluorescence was observed in blue channel (Fig. 2d). Thus, the fluorescence enhancement in the blue channel was indeed originated from **XQ-1** detecting endogenous $^1O_2$. In addition, the fluorescence in green channel displayed no evident change (Fig. 2e-2h, 2n), denoting that only limited dosage of $^1O_2$ was generated upon the stimulation of PMA. These results established that probe **XQ-1** is sensitive enough to detect the small dosage of endogenous $^1O_2$.

Next, probe **XQ-1** was applied for imaging of intracellular $^1O_2$ during the simulated PDT process. The 5-aminolevulinic acid (5-ALA) induced protoporphyrin IX (PpIX) was used as PS.[6f] PC12 cells were treated with 150 μg ml^{-1} 5-ALA for 12 h, and then stained with **XQ-1** for another 30 min. No background fluorescence was observed in the

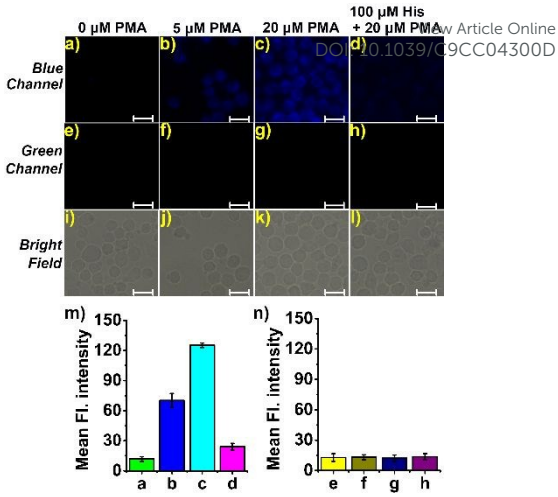

Fig. 2 The fluorescence image of probe **XQ-1** detecting endogenous $^1O_2$ in RAW 264.7 macrophage cells. (a)-(c): The fluorescence image in blue channel of the cells stained with 2 μM **XQ-1** in presence of 0 μM, 5 μM, and 20 μM PMA, respectively; (d): The fluorescence image in blue channel of the cells pre-treated with 100 μM His, and then stained with 2 μM **XQ-1** in the presence of 20 μM PMA; (e)-(h): The fluorescence imaging in green channel of the cells corresponding to (a)-(d); (i)-(l): The bright field images of the cells corresponding to (a)-(d); (m)-(n): Quantification of mean fluorescence intensity in (a)-(d) and (e)-(h), respectively. The scale bar in (a)-(l) is 20 μm.

blue channel and green channel (Fig. 3a,3d). Subsequently, the selected cell region was continuously irradiated by 405 nm laser, and the fluorescence imaging was acquired at different time interval. After irradiation for 150 s, the cells in the irradiated region showed intense fluorescence in the blue channel, while the cells in the unirradiated region displayed no fluorescence (Fig. 3b, 3h). In addition, no fluorescence was detected in the green channel (Fig. 3e, 3i). These denoted that only small dosage of $^1O_2$ was generated in the irradiated cells region at the early stage of PDT process. Upon continuous irradiation of the selected cells for 50 min, the fluorescence in the blue channel of the irradiated cells was significantly suppressed (Fig. 3c, 3h), whereas the fluorescence in the green channel of the irradiated cells became pretty brighter (Fig. 3f, 3i), indicative of a large dosage of $^1O_2$ being generated under the continuous irradiation. Notably, the unirradiated cells surrounding the irradiated cells region exhibited obvious fluorescence in the blue channel (Fig. 3c, 3g, 3h), implying small dosage of $^1O_2$ was generated in these cells. Owing to the radial diffusion distance of $^1O_2$ in an H_2O-incubated cells is only around 155 nm,[19] the generated $^1O_2$ was unable to diffuse from the irradiated region to the surrounding unirradiated region. Accordingly, the strong blue fluorescence in the unirradiated cells was apparently ascribed to the scatter light induced $^1O_2$. The fluorescent probe itself has the possibility to produce $^1O_2$ under irradiation, which may interfere the $^1O_2$ detection.[10a] This problem is frequently occurred in a commercially available $^1O_2$ probe Singlet Oxygen Sensor Green (SOSG).[20] To rule out this possibility, the PC12 cells were only incubated with **XQ-1**, and then were continuously irradiated with 405 nm laser for 50 min. No fluorescence was observed in the blue channel and green channel (Fig. S25), signifying that probe **XQ-1** itself cannot produce $^1O_2$ under irradiation. Therefore, during the PDT process, probe **XQ-1** can be used as a powerful tool to not only monitor $^1O_2$ in the irradiated cell region with a large concentration range, but also track the small dosage of $^1O_2$ in the unirradiated cell region with high sensitivity.

The colocalization experiments displayed that probe **XQ-1** was mainly localized in mitochondria (Fig. S26). This is presumably

because the negative mitochondrial membrane potential (Δψ) allows the positively charged probe to accumulate in mitochondria.[21] The cytotoxicity of probe **XQ-1** to PC12 cells was evaluated by a standard 3-(4,5-dimethylthiazol-2-yl)-2,5-diphenyl tetrazolium bromide (MTT) assay, and the results denoted that the cytotoxicity of the probe was relative low (The cell viabilities remained above 90% after incubation with 5 μM probe for 24 h) (Fig. S27).

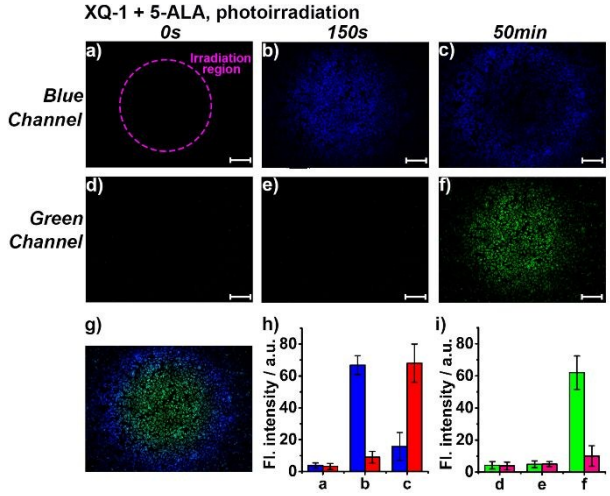

Fig. 3 Fluorescence imaging of $^1O_2$ during the simulated PDT process. The PC12 cell was pre-treated with 150 μg ml^{-1} 5-ALA for 12 hours, and then the cells were stained with 2 μM **XQ-1**. Upon continuously irradiating the selected cell region with 405 nm laser, the fluorescence images in the blue channel and green channel were acquired at 0 s (a, d), 150 s (b, e), and 50 min (c, f), respectively. (g): The overlay image of (c) and (f). (h): Quantification of mean fluorescence intensity in (a)-(c); the blue bar and red bar represent the mean fluorescence intensity of the irradiated cells and the surrounding unirradiated cells, respectively. (i): Quantification of mean fluorescence intensity in (d)-(f); the green bar and pink bar represent the mean fluorescence intensity of the irradiated cells and the surrounding unirradiated cells, respectively. The cycle in (a) represents the selected irradiated cell region. The scale bar in (a)-(f) is 150 μm.

In conclusion, we rationally constructed a novel fluorescent probe for selectively detecting $^1O_2$ on the basis of two-step cascade sensing reaction. Notably, upon introducing small dosage of $^1O_2$, the first step sensing reaction was occurred, and the probe displayed pronounced fluorescence enhancement in blue channel. As a result, the probe could detect $^1O_2$ with high sensitivity. However, upon further introducing a large dosage of $^1O_2$, the second step sensing reaction was set out. The fluorescence of the probe in blue channel gradually decreased, while the fluorescence in green channel emerged and progressively increased. Therefore, the probe could also detect $^1O_2$ with a large concentration range. The fluorescence imaging of intracellular $^1O_2$ during the simulated PDT process showed that the probe was able to monitor $^1O_2$ in the irradiated cell with a large concentration range. Moreover, the probe was sensitive enough to track the small dosage of $^1O_2$ in the surrounding unirradiated cell. Therefore, the probe will be employed as a versatile tool to not only monitor the efficacy of PDT treatment to the cancer, but also can track the adverse effect of the PDT treatment to the surrounding healthy cells.

This research was supported by the National Natural Science Foundation of China (21874059), and the Foundation of Key Laboratory of Sensor Analysis of Tumor Marker, Ministry of Education, Qingdao University of Science and Technology (No. SATM201807).

Notes and references

View Article Online
DOI: 10.1039/C9CC04300D

1. C. Schweitzer and R. Schmidt, *Chem. Rev.*, 2003, **103**, 1685.
2. P. Agostinis, K. Berg, K. A. Cengel, T. H. Foster, A. W. Girotti, S. O. Gollnick, S. M. Hahn, M. R. Hamblin, A. Juzeniene, D. Kessel, M. Korbelik, J. Moan, P. Mroz, D. Nowis, J. Piette, B. C. Wilson and J. Golab, *CA Cancer J. Clin.*, 2011, **61**, 250.
3. S. S. Lucky, K. C. Soo and Y. Zhang, *Chem. Rev.*, 2015, **115**, 1990.
4. (a) Y. Liu, X. Meng and W. Bu, *Coord. Chem. Rev.*, 2019, **379**, 82; (b) L. Cheng, C. Wang, L. Feng, K. Yang and Z. Liu, *Chem. Rev.*, 2014, **114**, 10869.
5. Y. Yang, Q. Zhao, W. Feng and F. Li, *Chem. Rev.*, 2013, **113**, 192.
6. (a) W. Hou, Y. Yuan, Z. Sun, S. Guo, H. Dong and C. Wu, *Anal. Chem.*, 2018, **90**, 14629; (b) S. K. Pedersen, J. Holmehave, F. H. Blaikie, A. Gollmer, T. Breitenbach, H. H. Jensen and P. R. Ogilby, *J. Org. Chem.*, 2014, **79**, 3079; (c) R. Ruiz-Gonzalez, R. Bresoli-Obach, O. Gulias, M. Agut, H. Savoie, R. W. Boyle, S. Nonell and F. Giuntini, *Angew. Chem. Int. Ed.*, 2017, **56**, 2885; (d) M. Sun, S. Krishnakumar, Y. Zhang, D. Liang, X. Yang, M. W. Wong, S. Wang and D. Huang, *Sens. Actuators, B*, 2018, **271**, 346; (e) K. Tanaka, T. Miura, N. Umezawa, Y. Urano, K. Kikuchi, T. Higuchi and T. Nagano, *J. Am. Chem. Soc.*, 2001, **123**, 2530; (f) S. Kim, T. Tachikawa, M. Fujitsuka and T. Majima, *J. Am. Chem. Soc.*, 2014, **136**, 11707; (g) J. Sun, B. Song, Z. Ye and J. Yuan, *Inorg. Chem.*, 2015, **54**, 11660.
7. (a) D. Song, S. Cho, Y. Han, Y. You and W. Nam, *Org. Lett.*, 2013, **15**, 3582; (b) R. P. Zanocco, R. Bresoli-Obach, S. Nonell, E. Lemp and A. L. Zanocco, *Plos One*, 2018, **13**.
8. K. Xu, L. Wang, M. Qiang, L. Wang, P. Li and B. Tang, *Chem. Commun.*, 2011, **47**, 7386.
9. H.-W. Liu, S. Xu, P. Wang, X.-X. Hu, J. Zhang, L. Yuan, X.-B. Zhang and W. Tan, *Chem. Commun.*, 2016, **52**, 12330.
10. (a) N. Hananya, O. Green, R. Blau, R. Satchi-Fainaro and D. Shabat, *Angew. Chem. Int. Ed.*, 2017, **56**, 11793; (b) X. H. Li, G. X. Zhang, H. M. Ma, D. Q. Zhang, J. Li and D. B. Zhu, *J. Am. Chem. Soc.*, 2004, **126**, 11543.
11. (a) K. K. Wang, J. C. Finlay, T. M. Busch, S. M. Hahn and T. C. Zhu, *J. Biophotonics*, 2010, **3**, 304; (b) I. Georgakoudi, M. G. Nichols and T. H. Foster, *Photochem. Photobiol.*, 1997, **65**, 135.
12. (a) M. J. Davies, *Biochem. Biophys. Res. Commun.*, 2003, **305**, 761; (b) E. W. Kellogg, III and I. Fridovich, *J. Biol. Chem.*, 1975, **250**, 8812; (c) M. Subramanian, Sreejayan, M. N. Rao, T. P. Devasagayam and B. B. Singh, *Mutat. Res.*, 1994, **311**, 249.
13. (a) H. S. Jung, J. H. Han, T. Pradhan, S. Kim, S. W. Lee, J. L. Sessler, T. W. Kim, C. Kang and J. S. Kim, *Biomaterials*, 2012, **33**, 945; (b) L. Long, L. Wang, Y. Wu, A. Gong, Z. Da, C. Zhang and Z. Han, *Chem. Asian J.*, 2014, **9**, 3291.
14. J. Aubry and B. Cazin, *Inorg. Chem.*, 1988, **27**, 2013.
15. H. H. Wasserman and J. R. Scheffer, *J. Am. Chem. Soc.*, 1967, **89**, 3073.
16. A. A. Ghogare and A. Greer, *Chem. Rev.*, 2016, **116**, 9994.
17. J. R. Kanofsky, H. Hoogland, R. Wever and S. J. Weiss, *J. Biol. Chem.*, 1988, **263**, 9692.
18. M. J. Steinbeck, A. Khan and M. Karnovsky, *J. Biol. Chem.*, 1993, **268**, 15649.
19. P. R. Ogilby, *Chem. Soc. Rev.*, 2010, **39**, 3181.
20. A. Gollmer, J. Arnbjerg, F. H. Blaikie, B. W. Pedersen, T. Breitenbach, K. Daasbjerg, M. Glasius and P. R. Ogilby, *Photochem. Photobiol.*, 2011, **87**, 671.
21. Z. Xu and L. Xu, *Chem. Commun.*, 2016, **52**, 1094.

View Article Online
DOI: 10.1039/C9CC04300D

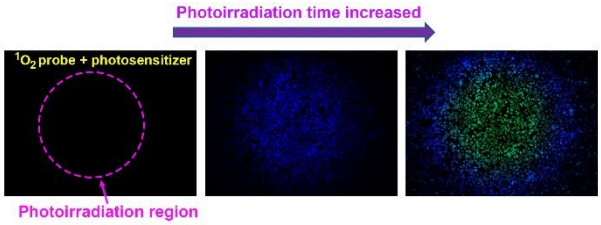

A novel fluorescent probe for detecting $^1O_2$ on the basis of two-step cascade reaction has been rationally constructed.